Journal of Power Sources 237 (2013) 172–177

Contents lists available at SciVerse ScienceDirect

Journal of Power Sources

journal homepage: www.elsevier.com/locate/jpowsour

Synthesis of porous NiO materials with preferentially oriented crystalline structures with enhanced stability as lithium ion battery anodes

Gil-Pyo Kim, Soomin Park, Inho Nam, Junsu Park, Jongheop Yi*

World Class University Program of Chemical Convergence for Energy & Environment, Institute of Chemical Processes, School of Chemical and Biological Engineering, College of Engineering, Seoul National University (SNU), Seoul 151-742, Republic of Korea

HIGHLIGHTS

- Porous NiO with preferentially oriented structure is synthesized through cathodic deposition.
- Agarose gel is used as a meditative template and conductive carbon sources.
- The composite films exhibit an enhanced reversible capacity and cycling stability as anode materials.
- The improvement is ascribed to the synergetic effects of unique structure between porous NiO and carbonaceous matrix.

GRAPHICAL ABSTRACT

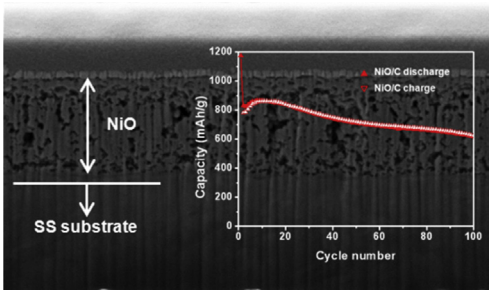

ARTICLE INFO

Article history:
Received 21 January 2013
Received in revised form
26 February 2013
Accepted 1 March 2013
Available online 21 March 2013

Keywords:
Agarose gel
Nickel oxide
Electrodeposition
Preferential growth
Lithium-ion battery

ABSTRACT

A simple strategy is described for the synthesis of nickel oxide embedded in a carbonaceous matrix (NiO/C) using a templated agarose gel thin film, in an attempt to produce an electrode with a large reversible capacity and long cycle stability. The as-prepared films are directly deposited onto stainless steel substrates from a solution of the Ni^{2+} precursors. Scanning electron microscopy images indicate that the as-synthesized NiO/C has a porous and interconnected structure. The results of X-ray diffraction and Fourier transform-infrared spectroscopy analyses confirm the preferential (111) growth of NiO and the presence of carbonaceous materials. As an anode material for lithium ion batteries, this novel structure plays a positive role in producing a material with a large reversible capacity, high conductivity, and long cyclic stability. The high reversible capacity is maintained at an elevated current density. Even after 100 cycles, the NiO/C anodes deliver more than 600 mAh g^{-1} at a current density of 718 mA g^{-1}, which is significantly higher than the capacity of commercial graphite anodes. The results indicate the existence of a synergetic effect between the porous NiO layers and the conductive matrix in the composite.

1. Introduction

Due to their high energy density and power density, lithium-ion batteries (LIBs) are one of the most promising candidates for use in energy storage and conversion devices. In particular, recent progress in the study of alternative anode materials for LIBs has stimulated rapid development in this field. Electrochemically active metal oxides, such as Co_3O_4 [1–3], NiO [4–6], Fe_2O_3 [7], and MnO_2 [8], and carbon-based composites thereof [9–11] have been exploited as the anode materials for LIBs. Although a variety of techniques including an in-situ reduction process [12], a sol–gel process [13], and chemical vapour

* Corresponding author. Tel.: +82 2 880 7438.
E-mail address: jyi@snu.ac.kr (J. Yi).

0378-7753/$ – see front matter © 2013 Elsevier B.V. All rights reserved.
http://dx.doi.org/10.1016/j.jpowsour.2013.03.046

deposition [14] have been widely used in the fabrication of the above-mentioned materials, electrodeposition is a particularly attractive technique, in that the coating mass, thickness, and morphology of the metal oxide thin film can be easily controlled by adjusting the applied current and bath composition [15,16]. In addition, the electrode can be directly synthesized onto a substrate without any complicated processing step involving the addition of a binder or an electrical conductor. Due to the different shrinkage or expansion properties between the deposited thin film and the substrate, however, peeling or cracking of the active material layers occur on the substrate, which are typically the result of the heat treatment used in the crystallization process, which can result in poor reversible capacity and electronic conductivity [17,18].

To achieve an enhanced structural electrochemical stability, numerous efforts have been devoted to the development of new types of templating techniques [19,20]. Biopolymer templates including cellulose [21], dextran-based polymers [22], and agarose [23] have been used in a variety of applications due to their ease of preparation, low cost, and environmental benignness, and the fact that they are freely soluble in water. Among the above-mentioned materials, agarose gels, with sub-micrometer porous network structures, have numerous applications for biological research [24] as well as serving as a promising organic template for the synthesis of porous metal oxides using the sol–gel method [24,25]. An agarose polymer matrix not only has an excellent film-forming ability on the substrate and is highly stable in an aqueous solution but also can effectively deliver metallic precursors to the interior of the gel [23], which could be used as a meditative template for the fabrication of highly mechanically stable metal oxide thin films by electrodeposition [23]. In addition, the electrodeposited metal hydroxide/agarose gel thin film can be readily converted into a well-dispersed metal oxide embedded on a carbonaceous matrix by heat treatment under nitrogen atmosphere [26,27]. The carbonaceous matrix effectively alleviates the volume expansion and aggregation of nanoparticles. Moreover, the carbonaceous layer can function as a highly conductive matrix, thus enabling good electrical contact with the metal oxide and can serve as a preventive measure against electrode pulverization. More importantly, during the electrodeposition process, the direction of diffusion of metallic precursors can be regulated by the applied electric field through the hydrogel, resulting in the isotropic crystal growth of the metal oxide [28]. The one-dimensional structure enables electrons to easily travel to the electrode/electrolyte interface.

Among the transition metal oxides, NiO is one of the promising anode materials for use in LIBs because of its high theoretical capacity (718 mAh g^{-1}) [29], which would be expected to meet the increasing demand for high performance LIBs. Practical applications, however, continue to be restrained by detrimental effects related to its structural and electrochemical properties, resulting from the pulverization of active materials by the large volume change that occurs during the cycling process. In this study, we demonstrate the use of agarose-mediated electrodeposition method as a simple strategy for the synthesis of preferentially grown nickel oxide embedded in a conducting carbonaceous matrix (NiO/C) as an advanced anode material for use in LIBs. The electrodeposited composites can efficiently utilize the combined merits of NiO with a preferred orientation and a carbonaceous matrix, resulting in superior electrochemical properties with a large reversible capacity, excellent cycling stability, and an enhanced conductivity as an anode material in LIBs. As a result, agarose gel-templated electrodeposition represents a promising procedure for the synthesis of inorganic–organic hybrid materials for energy storage applications.

2. Experimental

The NiO/C was prepared as follows. A 1% (w/v) solution of agarose powder was prepared in deionized (DI) water with vigorous stirring. The solution was heated to boiling using a microwave oven. For the preparation of agarose gel template, the above aqueous solution was then cast on stainless steel (SS) substrates (2×4 cm^2) by a dip-coating method, followed by a 4 h period of gelation at room temperature. The plating bath was comprised of 0.05 M of $Ni(NO_3)_2$ and 0.075 M of $NaNO_3$ in DI water. The electrodeposition was performed potentiostatically at −1.0 V (vs Ag/AgCl) for 300 s at room temperature. The agarose coated SS was employed as a working electrode. A Pt plate and Ag/AgCl were used as the counter electrode and reference electrode, respectively. After electrodeposition, the as synthesized films were rinsed with DI water and dried at room temperature for 24 h, followed a heat treatment at 350 °C for 2 h under a nitrogen atmosphere. For comparison, a pure NiO film without an agarose template was electrodeposited following the similar procedure without an agarose template for 300 s.

The NiO/C composite material was characterized by scanning electron microscopy (SEM, Carl Zeiss, SUPRA 55VP), focused-ion beam microscopy (FIB, Carl Zeiss, AURIGA), energy dispersive spectrometry (EDS, Bruker, Xflash5030 detector), X-ray diffraction (XRD, Rigaku, D/max-2200), and Fourier transform-infrared spectroscopy (FT-IR, Thermo Scientific, Nicolet 6700).

Electrochemical experiments were performed using a conventional coin cell (CR2032). The electrolyte solution was a 1 M $LiPF_6$ solution in ethyl carbonate and diethyl carbonate (1:1 by volume). The cells were assembled in an argon-filled glove box using as-prepared films as the working electrode. A lithium foil and microporous polypropylene were used as the counter electrode and separator, respectively. The galvanostatic discharge/charge measurements were conducted on a battery tester (WonA tech, WBCS3000) between 0.01 and 3.0 V with a constant current density of 718 mA g^{-1} (1 C). The electrochemical impedance spectroscopy (EIS) of the electrode was performed on an electrochemical workstation (WonA tech, ZIVE SP2). The frequency of EIS ranged from 0.01 Hz to 200 kHz at the open circuit potential.

3. Results and discussion

The SEM images and EDS atomic analysis data for the electrodeposited thin films after a heat treatment 350 °C for 2 h are shown in Fig. 1. Although the as-synthesized NiO film without an agarose gel template has a homogeneous dense and flat structure which is constructed by the aggregation of numerous small nanoscale-sized particles (Fig. 1a and b), a number of severe cracks are clearly observed. The cracked nature of the film is typically attributed to contraction and dehydration of hydroxide precursors by drying, during the heating process [17,30]. In contrast, in the case of an agarose gel template, the deposited film layer is relatively smooth and devoid of cracks (Fig. 1c and d). The electrodeposited NiO is homogeneously embedded in the carbonaceous matrix. Only minor amounts of NiO nanoparticles are observed on the surface as deposited film thickness increases to more than the thickness of the agarose gel template. From the above results, the carbonaceous matrix appears to efficiently act as a buffer region, preventing the cracking of deposits. To further confirm the elemental distribution of nickel and carbon in the deposits, EDS mapping was employed, and the results are shown in Fig. 1e and f. Both nickel and carbon are very uniformly distributed on the electrode surface. The average atomic ratio of Ni to C is about 61.3:38.7 at.%, respectively. This result demonstrates that a NiO/C composite with a high

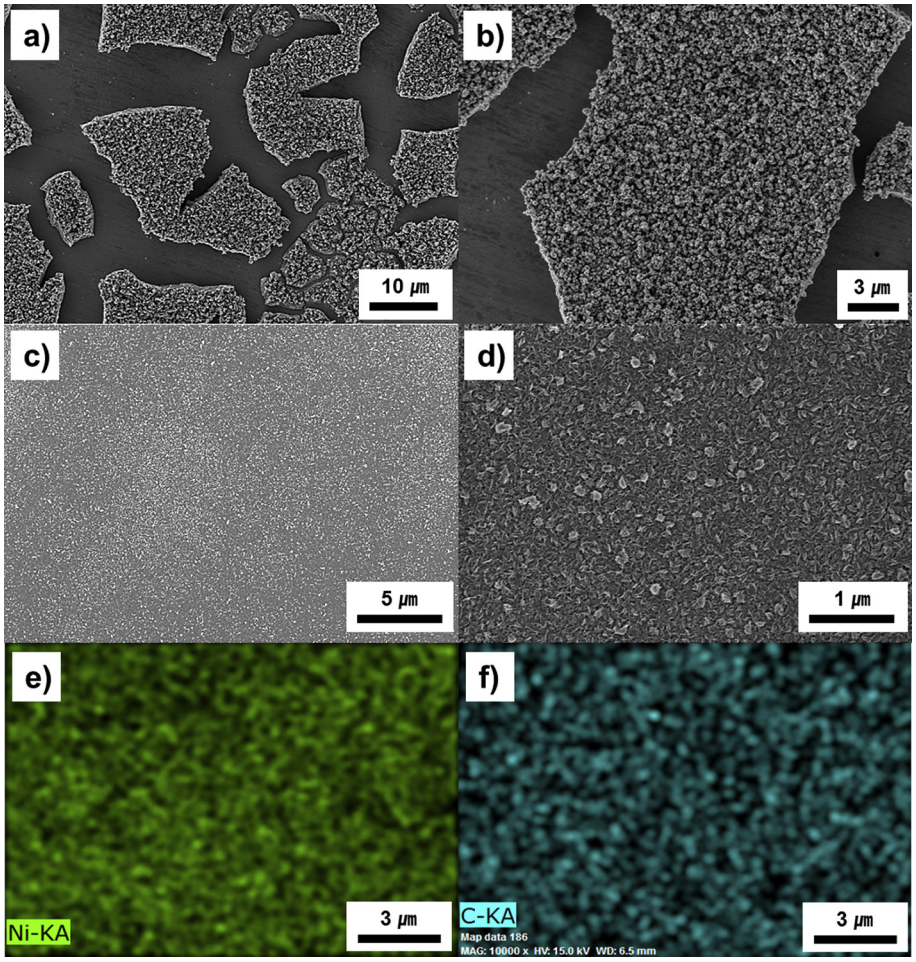

Fig. 1. SEM images of electrodeposited thin films; (a and b) NiO, (c and d) NiO/C after calcination at 350 °C for 2 h under a nitrogen atmosphere. EDS atomic analysis results for NiO/C films; (e) nickel and (f) carbon.

uniformity can be successfully prepared by electrodeposition using agarose gel template.

Cross-section SEM images of electrodeposited films after the heat treatment are shown in Fig. 2. The NiO films without template have a homogeneous densely-packed structure containing aggregates comprised of small nanoparticles and there are fewer voids in the deposited layer. Furthermore, the deposited NiO loses its structural rigidity, and consequently separates from the current collector. In contrast, NiO/C films not only have a smooth surface and uniform thickness but also adhere well to the substrate. More importantly, the interconnected porous structure is well-developed in the deposited layer, which facilitates the penetration of the electrolyte, thus permitting Li^+ ions to react more easily with more active sites. Moreover, this structure is beneficial for alleviating the large volume change that occurs during the cycling process. This result provides a clear demonstration to show that an agarose gel template plays an essential role in the formation of a porous NiO film with enhanced structural stability.

Fig. 3a displays XRD patterns for NiO and NiO/C films that were electrodeposited on a stainless steel substrate after calcination. These patterns clearly indicate the influence of the agarose gel template on the structural properties of the product. For the NiO film, the major diffraction lines correspond to (111), (200), and (220) crystalline of cubic NiO phase (JCPDS 47-1049). In the case of the NiO/C film, however, an unusually strong (111) and weak (222) diffraction peaks are observed. This result can be attributed to anisotropic ion diffusion inside the agarose gel [28]. The gel template is able to provide pathways for the precursor ions under an applied electric field, and Ni^{2+} ions linearly and compulsorily migrate inside the gels. Consequently, the ions are orientated in one direction, followed by a reduction process on the surface of the substrate. This is entirely different from findings of previous reports on the electrodeposition of NiO that were simply grown on bare substrates [16]. The small intensity of the (220) reflection can be attributed to the outward growth of NiO nanoparticulates from the agarose gel template. It should also be noted that the agarose gel template has a significant effect on the crystalline phase of the electrodeposited NiO. FT-IR measurements were carried out to gain insights into the chemical transformation that occurs when the agarose gel is converted into carbonaceous products through a heat treatment under a nitrogen atmosphere. IR spectra of the agarose gel before and after calcination are shown in Fig. 3b. Prior to the heat treatment, the characteristic peaks can be assigned to an −OH stretching vibration (around 3400 cm^{-1}). This band is correlated to the OH banding mode (1645 cm^{-1}), which arises from the hydroxyl groups of agarose and adsorbed water molecules. The bands around 2900 cm^{-1} are −CH stretching vibrations from the agarose gel. In the NiO/C composite, the characteristic peaks at 1700 and 1605 cm^{-1} are assigned to C═O and C═C vibrations corresponding to the carbonaceous matrix, respectively. Furthermore, the peaks at 1000–1450 cm^{-1} and the broad band at 3000–3750 cm^{-1} decrease significantly, indicating that dehydration occurred during the

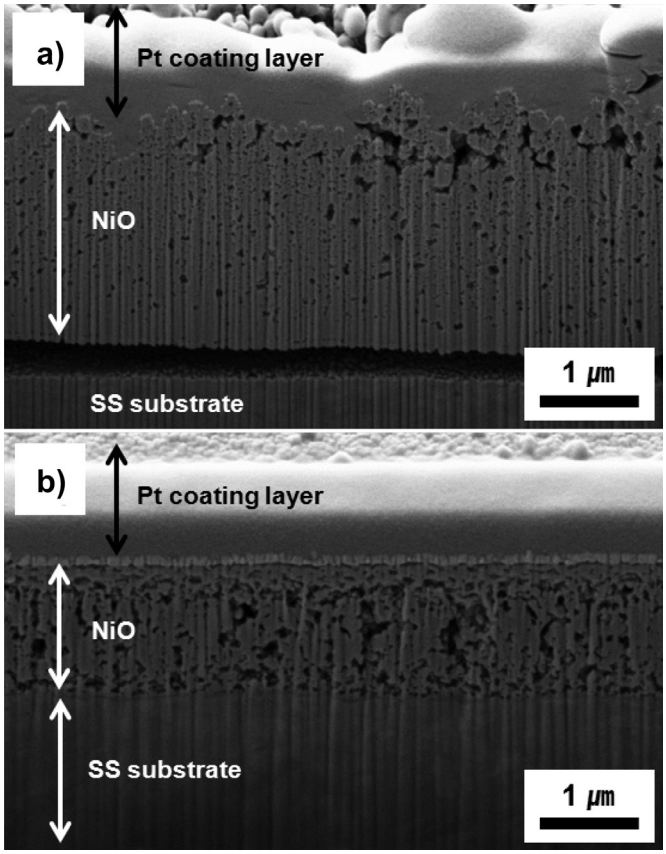

Fig. 2. Side views of SEM images of electrodeposited thin films; (a) pure NiO and (b) NiO/C films.

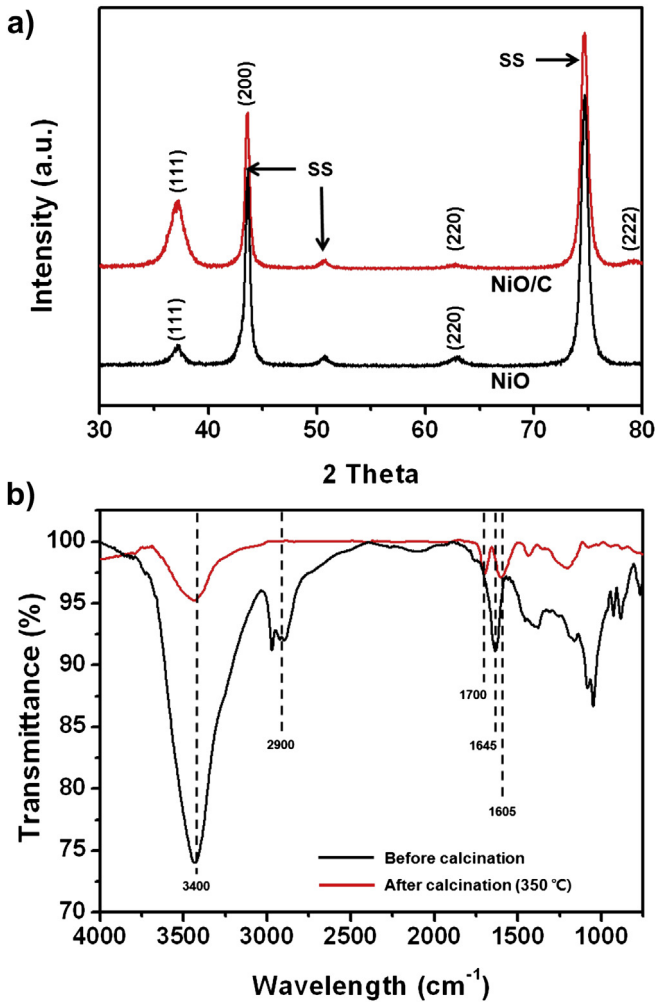

Fig. 3. (a) XRD spectra of NiO and NiO/C thin films after calcination and (b) IR spectra of an agarose gel before and after calcination at 350 °C for 2 h under a nitrogen atmosphere.

carbonization process [31–33]. This can be attributed to the fact that as synthesized $Ni(OH)_2$/agarose gel film is readily converted into a NiO/C composite by the carbonization process under a nitrogen environment at 350 °C for 2 h.

Fig. 4a and b show a comparison of the galvanostatic charge–discharge behaviour of bare NiO and NiO/C thin films at a constant current of 718 mA g^{-1} (1 C). The specific capacities were calculated based on the total mass of the active materials including the carbonaceous matrix. The first discharge and charge capacities are found to be 997 and 584 mAh g^{-1} for the pure NiO, corresponding to an initial columbic efficiency of 58.6% (Fig. 5a). By contrast, the NiO/C composite shows a large discharge capacity of 1140 mAh g^{-1} and a reversible capacity of 767 mAh g^{-1}, corresponding to an improved initial columbic efficiency of 67.3% (Fig. 5b). In addition, two potential regions can be observed in the discharge profile. Although a long voltage plateau is found around 0.6 V for both samples, which is the result of the reduction of NiO to Ni and the formation of a solid electrolyte interface (SEI) film, the potential region around 0.75 V corresponding to the formation of SEI and the Li-storage in carbonaceous matrix is not visible for the NiO film [34]. The introduction of a carbonaceous matrix indicates the existence of a synergetic effect that plays a role in the enhanced reversible capacity. The initial capacity loss could be attributed to the incomplete conversion reaction and irreversible lithium loss due to the formation of SEI [29]. The high reversibility and enhanced stability of the NiO/C composite film is even more strongly highlighted, as shown in Fig. 4c. The cyclic performance was evaluated at a current density of 1 C between 0.01 and 3.0 V. The reversible capacity of the pure NiO electrode rapidly drops to 203 mAh g^{-1} after 100 cycles, only a 35% retention of the initial charge capacity. In contrast, the NiO/C composite film exhibits a high reversible capacity of 604 mAh g^{-1} at a high level for up to 100 cycles, which is almost three times higher than that of the NiO film. The retention of capacity is maintained above 78%. More importantly, the reversible capacity of NiO/C electrode increases slightly from the 2nd cycle and reaches 864 mAh g^{-1} at the 10th cycle. These results can be attributed to gradual activation by the formation of a stable SEI within the interconnected porous structure of the NiO during the first several cycles [29,35]. The structure appears to reach a stabilized state, which is consistent with the observed extra capacity until 10 cycles. The rate capability of NiO/C was also demonstrated at various rates from 0.5 to 2 C, as shown in Fig. 4d. The sustained nature of the composite film is clearer at a high current density. Upon increasing the current density to 1, 1.5, and 2 C, the NiO/C is still able to deliver a discharge capacity of 693, 621, and 563 mAh g^{-1}, respectively. It is obvious that, although a current increase leads to a gradual decrease in reversible capacity, the current density has little impact on the overall process. Based on the above results, the high reversibility and excellent cycling stability can be explained as follows: 1) the interconnected porous NiO structure could be favourable for Li^+ diffusion to more active sites. 2) The sufficient void volume of the structure helps to accommodate the volume expansion. 3) The carbonaceous matrix prevents

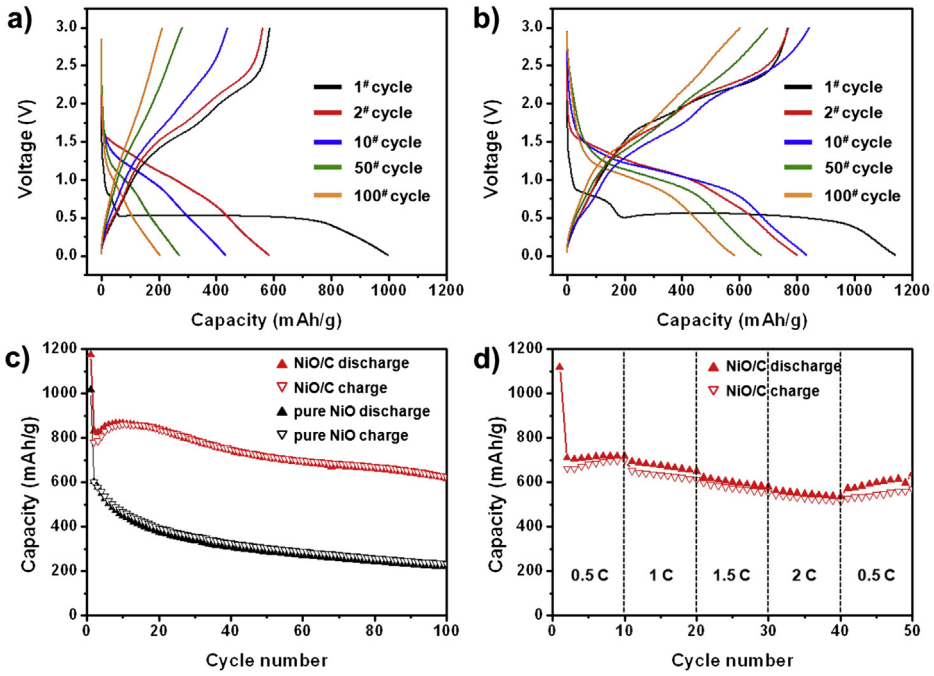

Fig. 4. Electrochemical performance test of electrodeposited films; charge/discharge curves of (a) NiO film and (b) NiO/C film, (c) cycleability of NiO and NiO/C films with a current density of 718 mA g^{-1} (1 C), and (d) rate capability test of the NiO/C film.

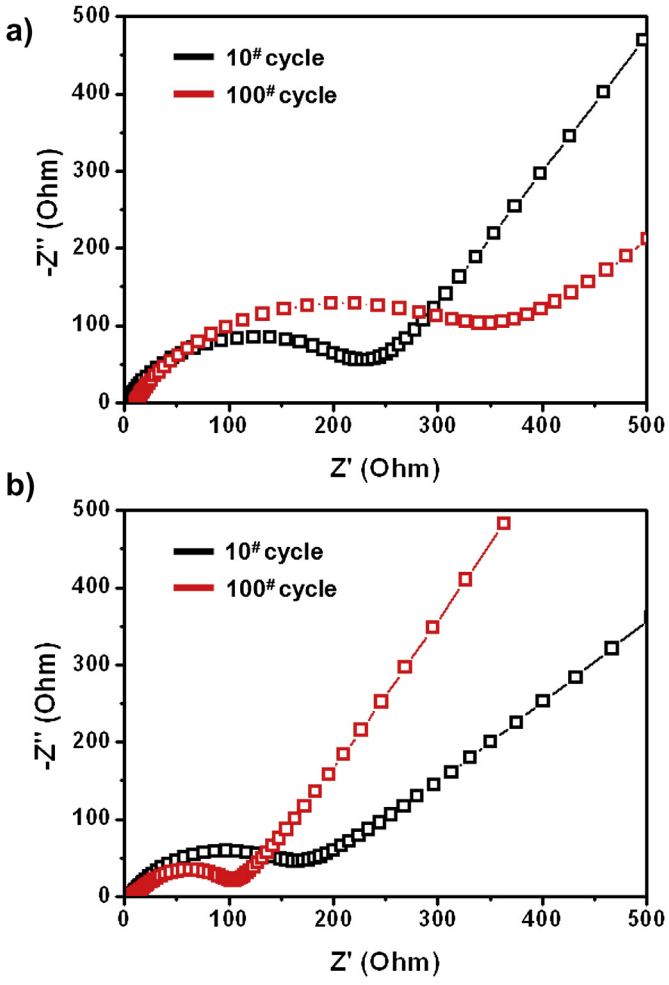

Fig. 5. Impedance comparison curves; (a) NiO films and (b) NiO/C film.

aggregation and the electrical isolation of active materials, and preserves the integrity of the overall electrode from disconnecting the current collector as an elastic buffer space.

In order to gain further insights into the role of the carbonaceous matrix and the preferential orientated structure as a provider for an electrical conductive network, EIS measurements of the NiO and NiO/C electrodes were conducted after the 10th and 100th cycles, as shown in Fig. 5. Nyquist plots indicate that the diameter of the semicircle for NiO/C film in the medium frequency region is much smaller than that of NiO, indicating that NiO/C composite electrode possesses lower charge transfer resistances at the 10th cycle [36]. After cycling, the impedance data at the end of 100 cycles shows that the diameter of the semicircle in the medium frequency region for NiO is much larger than that for the electrode before cycling, indicating increased charge transfer resistances (Fig. 5a). During continued cycling, it is possible that the NiO materials could undergo a large volume change by the electrochemical conversion reactions, leading to mechanical stress and subsequent pulverization of the active layers, followed by electrical isolation and contact loss within the as-synthesized electrode. In contrast, it can be clearly seen that the semicircle for the NiO/C composite is smaller than that for the electrode before cycling (Fig. 5b). This behaviour indicates that NiO embedded in a carbonaceous matrix is favourable for the formation of a stable SEI film. In addition, the intercept at the real axis at a high frequency, corresponding to the ohmic resistance, is nearly constant after cycling, which suggests good contact between the current collector and the electrode, as well as the structure integrity of the NiO/C electrode (Fig. 5b) [37]. To further confirm the structure integrity of the as-synthesized films, the evolution of the morphology and structure of NiO and NiO/C were investigated, as shown in Fig. 6. The SEM image of the NiO film after 100 cycles clearly shows that the electrode suffers from severe cracking and that the active layers have become pulverized. Subsequently, the deposited NiO deteriorates with most of the film being peeled off from the substrate. In contrast, the NiO with a carbonaceous matrix do not suffer from observable morphological changes and retains its structural integrity with only a slight

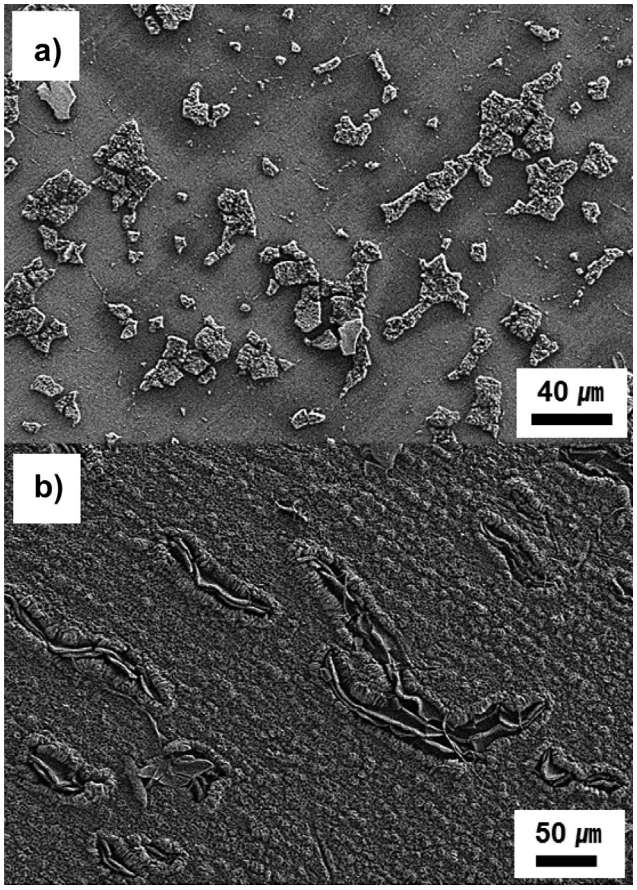

Fig. 6. SEM images of electrodes after 100 cycles; (a) NiO and (b) NiO/C.

deformation. On the basis of the above results, the improved electrochemical performance of the NiO/C composite could be reasonably attributed to the advantageous combination of preferentially grown NiO and a carbonaceous matrix. The matrix induces the formation of stable SEI layers and improves the conductivity of the composite. The flexibility of the matrix can maintain structural integrity by suppressing the pulverization of active materials and by accommodating volume expansion that occurs during the cycle process. Moreover, the preferentially oriented crystalline material can assist electron transport between the substrate and electrolyte, thereby contributing to the enhanced electrical conductivity and cycleability of the product.

4. Conclusions

A simple strategy for fabricating porous NiO/C composite films by agarose-gel templated electrodeposition is reported. The structures are composed of preferentially orientated (111) crystalline substances. The resulting composite films can be directly used for an LIB anode material. The as-synthesized NiO/C exhibits a significantly improved cycle stability, reversible capacity, and electrical conductivity, compared with bare NiO films, which is primarily attributed to the synergistic effect of the conductive carbonaceous matrix and the preferentially grown NiO with an interconnected porous structure. The present synthetic protocol opens up new opportunities for the synthesis of other materials with promising applications in supercapacitors and photocatalysts.

Acknowledgements

This research was supported by WCU (World Class University) program through the National Research Foundation of Korea funded by the Ministry of Education, Science and Technology (R31-10013).

References

[1] W.Y. Li, L.N. Xu, Adv. Funct. Mater. 15 (2005) 851–857.
[2] N. Du, H. Zhang, B. Chen, J.B. Wu, X.Y. Ma, Z.H. Liu, Y.Q. Zhang, D. Yang, Z.H. Huang, J.P. Tu, Adv. Mater. 19 (2007) 4505–4509.
[3] W.L. Yao, J. Yang, J.L. Wang, Y. Nuli, J. Electrochem. Soc. 155 (2008) A903–A908.
[4] B. Varghese, M.V. Reddy, Z. Yanwu, C.S. Lit, T.C. Hoong, G.V.S. Rao, B.V.R. Chowdari, A.T.S. Wee, C.T. Lim, C.H. Sow, Chem. Mater. 20 (2008) 3360–3367.
[5] X.H. Huang, J.P. Tu, X.H. Xia, X.L. Wang, J.Y. Xing, L. Zhang, Y. Zhou, J. Power Sources 188 (2009) 588–591.
[6] B. Wang, J.L. Cheng, Y.P. Wu, D. Wang, D.N. He, Electrochem. Commun. 23 (2012) 5–8.
[7] C.Z. Wu, P. Yin, X. Zhu, C.Z. OuYang, Y. Zie, J. Phys. Chem. B 110 (2006) 17806–17812.
[8] J.Z. Zhao, Z.L. Tao, J. Liang, J. Chen, Cryst. Growth Des. 8 (2008) 2799–2805.
[9] X.H. Huang, J.P. Tu, C.Q. Zhang, J.Y. Xiang, Electrochem. Commun. 9 (2007) 1180–1184.
[10] N. Jayaprakash, W.D. Jones, S.S. Moganty, L.A. Archer, J. Power Sources 15 (2012) 53–58.
[11] J. Shao, J. Zhang, J. Jiang, G. Zhou, M. Qu, Electrochim. Acta 15 (2011) 7005–7011.
[12] H. Kim, D.-H. Seo, S.-W. Kim, J. Kim, K. Kang, Carbon 49 (2011) 326–332.
[13] M. Gao, X. Chen, H. Pan, L. Xiang, F. Wu, Y. Liu, Electrochim. Acta 55 (2010) 9067–9074.
[14] I. Lahiri, S.-M. Oh, J.Y. Hwang, C. Kang, M. Choi, H. Jeon, R. Banerjee, Y.-K. Sun, W. Choi, J. Mater. Chem. 21 (2011) 13621–13626.
[15] Y. Tan, S. Srinivasan, K.S. Choi, J. Am. Chem. Soc. 127 (2005) 3596–3599.
[16] Y.F. Yuan, X.H. Xia, J.B. Wu, J.L. Yang, Y.B. Chen, S.Y. Guo, Electrochem. Commun. 12 (2010) 890–893.
[17] I. Paseka, Electrochim. Acta 47 (2001) 921–931.
[18] M. Saitou, S. Oshiro, Y. Sagawa, J. Appl. Phys. 104 (2008), 093518–093518-4.
[19] S.A. Davis, M. Breulmann, K.H. Rhodes, B. Zhang, S. Mann, Chem. Mater. 13 (2001) 3218–3226.
[20] S. Shinkai, K.J.C. van Brommel, A. Friggeri, Angew. Chem. Int. Ed. 42 (2003) 980–999.
[21] E. Dujardin, S.J. Mann, Mater. Chem. 13 (2003) 696–699.
[22] S. Polarz, B. Smarsly, L. Bronstein, M. Antonietti, Angew. Chem. Int. Ed. 40 (2001) 4417–4421.
[23] X. Shen, X. Chen, J.-H. Liu, X.-J. Huang, J. Mater. Chem. 19 (2009) 7687–7693.
[24] X. Wang, C.E. Egan, M. Zhou, K. Prince, D.R.G. Mitchell, R.A. Caruso, Chem. Commun. 29 (2007) 3060–3062.
[25] J.F. Zhou, M.F. Zhou, R.A. Caruso, Langmuir 22 (2006) 3332–3336.
[26] K.K.R. Datta, B. Srinivasan, H. Balaram, M. Eswaramoorthy, J. Chem. Sci. 120 (2008) 579–586.
[27] M. Sevilla, A.B. Fuertes, Carbon 47 (2009) 2281–2289.
[28] J. Watanabe, M. Akashi, J. Biomater. Sci. Polym. Ed. 19 (2008) 1625–1635.
[29] Y. Huang, X. Huang, J. Lian, D. Xu, L. Wang, X. Zhang, J. Mater. Chem. 22 (2012) 2844–2847.
[30] S. Arai, T. Saito, M. Endo, J. Electrochem. Soc. 154 (2007) D530–D533.
[31] I.F. Nata, S.S.-S. Wang, T.-M. Wu, C.-K. Lee, Soft Matter 8 (2012) 3522–3525.
[32] S.-H. Teng, P. Wang, H.-E. Kim, Mater. Lett. 63 (2009) 2510–2512.
[33] L. Kong, X. Lu, X. Bian, W. Zhang, C. Wang, W. Wang, X. Guo, Y. Yang, ACS Appl. Mater. Interfaces 3 (2011) 35–42.
[34] R. Yang, Z. Wang, J. Liu, L. Chen, Electrochem. Solid-State Lett. 7 (2004) A496–A499.
[35] L. Tao, J. Zai, K. Wang, Y. Wan, H. Zhang, C. Yu, Y. Xiao, W. Qian, RSC Adv. 2 (2012) 3410–3415.
[36] Y.J. Mai, J.P. Tu, C.D. Gu, X.L. Wang, J. Power Sources 209 (2012) 1–6.
[37] X. Jia, Z. Chen, A. Suwarnasarn, L. Rice, X. Wang, H. Sohn, Q. Zhang, B.M. Wu, F. wei, Y. Lu, Energy Environ. Sci. 5 (2012) 6845–6849.